Interaction of Scorpion α-Toxins with Cardiac Sodium Channels: Binding Properties and Enhancement of Slow Inactivation

Haijun Chen and Stefan H. Heinemann

From the Research Unit Molecular and Cellular Biophysics, Medical Faculty of the Friedrich Schiller University Jena, D-07747 Jena, Germany

ABSTRACT The effects of the scorpion α-toxins Lqh II, Lqh III, and LqhαIT on human cardiac sodium channels (hH1), which were expressed in human embryonic kidney (HEK) 293 cells, were investigated. The toxins removed fast inactivation with EC_{50} values of <2.5 nM (Lqh III), 12 nM (Lqh II), and 33 nM (LqhαIT). Association and dissociation rates of Lqh III were much slower than those of Lqh II and LqhαIT, such that Lqh III would not dissociate from the channel during a cardiac activation potential. The voltage dependence of toxin dissociation from hH1 channels was nearly the same for all toxins tested, but it was different from that found for skeletal muscle sodium channels (μI; Chen et al., 2000). These results indicate that the voltage dependence of toxin binding is a property of the channel protein. Toxin dissociation remained voltage dependent even at high voltages where activation and fast inactivation is saturated, indicating that the voltage dependence originates from other sources. Slow inactivation of hH1 and μI channels was significantly enhanced by Lqh II and Lqh III. The half-maximal voltage of steady-state slow inactivation was shifted to negative values, the voltage dependence was increased, and, in particular for hH1, slow inactivation at high voltages became more complete. This effect exceeded an expected augmentation of slow inactivation owing to the loss of fast inactivation and, therefore, shows that slow sodium channel inactivation may be directly modulated by scorpion α-toxins.

KEY WORDS: patch clamp • *Leiurus quinquestriatus hebraeus* • cardiac muscle • skeletal muscle • receptor site 3

INTRODUCTION

Voltage-gated Na^+ channels play a major role in rapid electrical signaling in excitable cells. They are modulated by a variety of toxins, which bind to various sites at the channel protein (Catterall, 1992; Gordon, 1997). The scorpion α-toxins are thought to bind to receptor site 3 (Catterall, 1992) that is partially formed by amino acid residues in the extracellular linker between segments S3 and S4 in the fourth homologous domain (D4) of the channel protein (Rogers et al., 1996; Benzinger et al., 1997, 1998). The extracellular regions between segments S5 and S6 in domains D1 and D4 are also discussed to contribute to receptor site 3 (Thomsen and Catterall, 1989). The major effects of scorpion α-toxins are a remarkable slowing of fast inactivation of Na^+ channels and slight modifications of the voltage dependence of channel activation. The effect of the extracellular toxin binding to inactivation, which is mainly mediated by the intracellular linker between domains D3 and D4 (West et al., 1992), is thought to be exerted via a coupling to the voltage-sensing S4 segment. In this sense, scorpion α-toxins can be considered a part of a large family of gating-modifying toxins that bind to the extracellular loops between S3 and S4 and that modify the voltage-dependent gating of the structurally related calcium (ω-grammotoxin; McDonough et al., 1997) and potassium (e.g., hanatoxin; Swartz and Mackinnon, 1997; Li-Smerin and Swartz, 1998, 2000; Li-Smerin et al., 1999; Winterfield and Swartz, 2000) channels. Therefore, a detailed study of toxin–channel interactions may also shed further light on the molecular mechanism of ion channel function.

As scorpion α-toxins remarkably slow down fast inactivation of Na^+ channels, they prolong the action potentials of excitable cells. As a consequence, these toxins may kill animals by inducing paralysis and arrhythmia (Hille, 1992). The exact mechanism can only be understood when the effects of several toxins of one scorpion species on various Na^+ channel subtypes are compared. Therefore, we examine here the effects of Lqh II, Lqh III, and LqhαIT, which are representatives of the subfamilies of α-toxins from the Israeli yellow scorpion *Leiurus quinquestriatus hebraeus*, namely classical α-toxins, α-like toxins, and α-toxins (Gordon et al., 1998), on human cardiac sodium channels (hH1).[1] The results are compared with previously published data on rat skeletal

H. Chen's present address is Section of Developmental Biology and Biophysics, Department of Pediatrics and Cellular and Molecular Physiology, Boyer Center for Molecular Medicine, Yale University School of Medicine, New Haven, CT 06536-0812.

Address correspondence to Dr. Stefan H. Heinemann, Research Unit Molecular and Cellular Biophysics, Medical Faculty of the Friedrich Schiller University Jena, Drackendorfer Strasse 1, D-07747 Jena, Germany. Fax: 49-3641-304-542; E-mail: stefan.h.heinemann@uni-jena.de

muscle sodium channels (μI; Chen et al., 2000) to infer about the physiological consequences of these α-toxins.

The binding of scorpion α-toxins to mammalian Na^+ channels has been shown to be voltage dependent, which means that the affinity of scorpion α-toxins to Na^+ channels is decreased during depolarization (Catterall, 1992; Rogers et al., 1996; Chen et al., 2000), but the source of this decreased affinity is not yet known. LqTx and ATX II (toxin from sea anemone *Anemonia sulcata*) partially lose their effect on fast inactivation of Na^+ channels after depolarization in a way that suggests a coupling to channel activation (Rogers et al., 1996). However, it is not clear whether there is a direct link to activation or a rather indirect link by means of coupled processes such as fast or slow inactivation. Our previous report on μI Na^+ channels (Chen et al., 2000) showed that the three scorpion α-toxins Lqh II, Lqh III, and LqhαIT dissociate from the channel in a voltage-dependent way in a voltage range where both activation and fast inactivation are expected to be saturated. This leaves open the question regarding the molecular mechanism underlying the voltage-induced toxin dissociation. In addition, it was found that the toxins tested share the same voltage dependence of dissociation, suggesting that this decreased affinity for scorpion α-toxins may be determined only by the channel property. Here, we test this hypothesis by examining a different cloned channel type.

In particular, we address the question on whether or not there is a coupling between α-toxin binding to Na^+ channels and slow inactivation. Besides the fast inactivation that is largely mediated by the cytosolic linker between domains D3 and D4 according to a hinged-lid mechanism (West et al., 1992), Na^+ channels can undergo inactivation at slower time scales, which is best characterized by very slow recovery from inactivation on the order of a minute at resting voltages (e.g., Rudy, 1978). Slow inactivation appears to be structurally separate from fast inactivation because it remains intact after fast inactivation was removed completely with α-chymotrypsin (Valenzuela and Bennett, 1994). However, it can be enhanced when fast inactivation is removed by inducing mutations in the fast inactivation structure (isoleucine, phenylalanine, and methionine [IFM] motif replaced by QQQ; Featherstone et al., 1996; Richmond et al., 1998). Unlike fast inactivation of Na^+ channels, slow inactivation seems to involve rather complex conformational changes of the channel protein. This notion is supported by several studies reporting on effects on slow inactivation by mutagenesis of Na^+ channels at very different locations in the channel protein, particularly interesting being those mutations that are linked to inherited human diseases such as myotonia (Balser et al., 1996; Cummins and Sigworth, 1996; Hayward et al., 1997; Richmond et al., 1997; Wang and Wang, 1997; Vilin et al., 1999; Mitrovic et al., 2000). A recent study shows that slow inactivation of Na^+ channels is even linked to structural rearrangements in the pore region (Ong et al., 2000).

As scorpion α-toxins at least partially remove fast inactivation of Na^+ channels, it is reasonable to assume that scorpion α-toxins enhance the slow inactivation of Na^+ channels. However, it is not easy to examine the effects of scorpion α-toxins on slow inactivation of Na^+ channels, because many scorpion α-toxins, like LqTx (Rogers et al., 1996), rapidly dissociate from Na^+ channels during relatively long and high depolarizations, which are necessary to induce steady-state slow inactivation. In these cases, effects of scorpion α-toxins on slow inactivation of Na^+ channels are expected to be negligible. However, the toxins used here, particularly Lqh III, interact with μI and also with hH1 Na^+ channels very strongly, providing a possibility to study the toxin action on slow inactivation without considerable toxin dissociation.

MATERIALS AND METHODS

Cell Culture

Human embryonic kidney (HEK) 293 cells (CAMR) were stably transfected with hH1 sodium channel α subunits (Gellens et al., 1992) according to the methods described previously (Chen et al., 2000), and the resulting HEK 293_hH1 cells were obtained. The cell lines HEK 293_hH1 and HEK 293_μI (Chen et al., 2000) were maintained in DME, supplemented with 10% FCS in a 5% CO_2 incubator.

Electrophysiological Measurements

Whole-cell voltage clamp experiments were performed as described previously (Chen et al., 2000). Patch pipets with resistances of 0.9–2.0 MΩ were used. The series resistance was compensated for by >80% to minimize voltage errors and cells with access resistance above 5 MΩ were discarded. A patch-clamp amplifier EPC9 was operated by Pulse+PulseFit software (both HEKA Elektronik). Leak and capacitive currents were corrected with a p/n method. Currents were low-pass filtered at 5 kHz and sampled at a rate of 25 kHz. All experiments were performed at 20 ± 2°C. The patch pipets contained the following: 35 mM NaCl, 105 mM CsF, 10 mM EGTA, and 10 mM HEPES, pH 7.4 with CsOH. The bath solution contained the following: 150 mM NaCl, 2 mM KCl, 1.5 mM $CaCl_2$, 1 mM $MgCl_2$, 5 mM glucose, and 10 mM HEPES, pH 7.4 with NaOH. Lqh III (Sautiere et al., 1998) and LqhαIT (Eitan et al., 1990) were obtained from Latoxan, and Lqh II (Sautiere et al., 1998) was provided by Dr. D. Gordon (Tel Aviv University, Tel Aviv, Israel). The application of toxins was performed with an application pipet as described previously (Chen et al., 2000).

Data analysis was performed using PulseFit (HEKA Elektronik) and IgorPro (WaveMetrics) running on Macintosh computers. All data were presented as mean ± SEM (n = number of independent experiments) unless stated otherwise. Two-tailed t tests were used to check for significant differences between two groups of data.

[1]*Abbreviations used in this paper:* HEK, human embryonic kidney cells; hH1, human cardiac sodium channel; IFM, isoleucine, phenylalanine, and methionine; μI, rat skeletal muscle sodium channel; rBII, rat brain sodium channel II.

Current-Voltage Relationships

From a holding potential of −120 mV, test depolarizations in the range from −80 to +70 mV were applied at time intervals of 6 s. The peak currents were measured during the test pulses and then fitted as a function of the test voltage (V) with an activation model assuming three independent gating units and a single-channel conductance obeying the Goldman-Hodgkin-Katz equation:

$$I(V) = \Gamma V \frac{1 - e^{-(V - E_{rev})/25\ \mathrm{mV}}}{1 - e^{-V/25\ \mathrm{mV}}} \frac{1}{[1 + e^{-(V - V_m)/k_m}]^3} . \quad (1)$$

Γ is the conductance, and E_{rev} is the reversal potential. The last term describes the open probability of the channels, characterized by the voltage of half-maximal activation per subunit, V_m, and the slope factor, k_m.

Steady-State Fast and Slow Inactivation

For steady-state fast inactivation, conditioning pulses of 500-ms duration ranging between −140 and −30 mV were applied before available channels were assayed with a short depolarizing pulse to −20 mV. The resulting inward currents were normalized to the maximal current predicted by the data fit with Eq. 2. The voltage dependence of steady-state fast inactivation was described with a Boltzmann function of first order, characterized by the half-maximal voltage of fast inactivation, V_{hf}, and the corresponding slope factor, k_{hf}:

$$I_{norm}(V) = a_0 + a_1 / \{1 + \exp[(V - V_{bf})/k_{bf}]\} , \quad (2)$$

where a_0 is an offset, and a_1 is the amplitude. When fitting steady-state fast inactivation without toxins, $a_0 = 0$ and $a_1 = 1$.

For steady-state slow inactivation, the membrane potential was stepped from holding potential to the first 10-ms test pulse (*S1*) at 0 mV, and then recovered from inactivation for 5 ms at −120 mV. The second 30-ms test pulse (*S2*) to 0 mV was used to elicit Na^+ currents (I_{S2}) after inducing steady-state slow inactivation by 60-s prepulses at several voltages and subsequent recovery from fast inactivation for 50 ms at −140 mV (see Figs. 7 A and 9 A). The first test pulse was used to monitor the full toxin effect before each prepulse voltage and to normalize the peak current changes occurring during the experiment. The membrane potential held at −140 mV for at least 40 s between each recording allowed to completely recover from slow inactivation. The peak current I_{S2} was normalized to the peak current I_{S1} and was plotted as a function of the prepulse voltage (see Figs. 7 B and 9 B). The voltage dependence of slow inactivation was fitted with Eq. 2, characterized by the half-maximal voltage of slow inactivation, V_{hs}, and the corresponding slope factor, k_{hs}.

Degree of Fast Inactivation

The degree of fast inactivation was assayed by measuring the peak current as well as the mean current level between 4.5 and 5 ms after the start of the depolarization. This ratio $I_{5\ ms} / I_{peak}$ gives an estimate of the probability for the channels not to be inactivated after 5 ms: a value of zero represents complete inactivation in 4.5 ms; a value of one, no inactivation.

Kinetics of Fast and Slow Inactivation

Kinetics of fast inactivation was quantified by double-exponential functions to the decaying section of the Na^+ currents:

$$I(t) = a_{DC} + a_f \exp(-t/\tau_f) + a_s \exp(-t/\tau_s) . \quad (3)$$

a_{DC} is the noninactivating current amplitude, a_f and a_s are the amplitudes, and τ_f and τ_s are the time constants of the fast and the slow component, respectively.

The development of slow inactivation was examined with a two-pulse protocol. After the first test pulse (*S1*), the membrane potential was held for conditioning pulses with increasing durations (60 ms to 104 s). The second test pulse (*S2*) was used to monitor how much current (I_{S2}) was available after recovery from fast inactivation (see Fig. 8 A). The normalized currents I_{S2}/I_{S1} provided information about how many channels entered slow inactivation during the conditioning pulse. Plotting the ratio I_{S2}/I_{S1} as the function of the conditioning pulse durations yielded the time constants of the development of slow inactivation, based on fits with double-exponential functions (Eq. 3).

The recovery from slow inactivation was investigated with a similar two-pulse protocol. The first test pulse (*S3*) was used to elicit Na^+ current (I_{S3}). Subsequent depolarization to 0 mV for 60 s was used to induce steady-state slow inactivation. After recovering at −140 mV with increasing durations, the second test pulse (*S4*) was used to record the current (I_{S4}; see Fig. 8 B). Recovery time constants were obtained with Eq. 3 by fitting the ratio I_{S4}/I_{S3} versus recovery duration.

Dose–Response Curves of Toxin Effects on Fast Inactivation

The dose dependence for toxin-induced removal of fast inactivation was measured by plotting the ratio $I_{5\ ms}/I_{peak}$ at 0 mV as a function of toxin concentration, which is described with the Hill equation:

$$I_{5\,ms}/I_{peak}(0\ \mathrm{mV}) = a_o + (a_1 - a_0)/[1 + (EC_{50}/[toxin])^h], \quad (4)$$

where h is the Hill coefficient, [toxin] is the toxin concentration, and a_0 is the offset. The amplitude, a_1, provides the maximal value of the ratio $I_{5\ ms}/I_{peak}$ at 0 mV indicating the expected maximal effect of the toxin on fast inactivation. EC_{50} provides a measure for the concentration of half-maximal fast inactivation inhibition. For data fits, the a_0 values always were held at the values obtained under control conditions. Errors for EC_{50}, a_1, and h were obtained from these fits with the Igor Program (WaveMetrics), considering the SEM values of the individual data points for the weighting.

Toxin Dissociation and Association Kinetics

Dissociation kinetics was measured with double-pulse protocols. A conditioning dissociation pulse (from +20 to +180 mV) with increasing durations was applied, returning to −120 mV for 50 ms to recover channels from fast inactivation. Na^+ current was then elicited with a 30-ms test pulse to −20 mV. The holding potential of −120 mV ascertained maximum toxin rebinding. The extent of removal of fast inactivation was assayed with the ratio $I_{5\ ms}/I_{peak}$. The average values of $I_{5\ ms}/I_{peak}$ from several experiments were plotted as a function of the dissociation durations. Single-exponential fits revealed the time constants (τ_{off}). The time course of toxin dissociation was determined in the range of membrane voltages. Plotting τ_{off} as the function of the dissociation voltage produced the voltage-dependent dissociation curves. Single-exponential fits (Eq. 5) revealed the voltage dependence:

$$\tau(V) = (\tau_o - \tau_\infty) \exp(-ze_o/kT) + \tau_\infty , \quad (5)$$

where τ_0 is the time constant at 0 mV, e_0 is the unitary electron charge, and z is the apparent gating valence (gating charge, ze_0). In some cases, a steady-state component (τ_∞) was necessary to describe the data. The fit provides the slope factor, which indicates

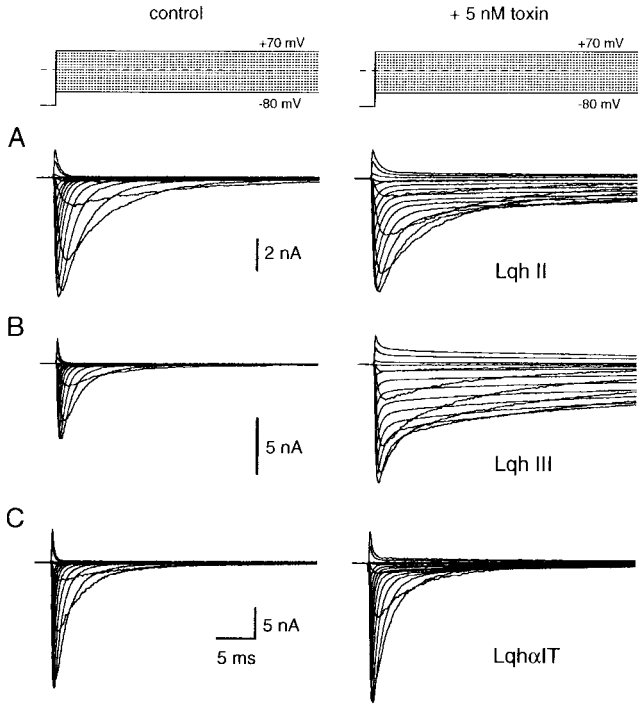

FIGURE 1. Lqh II, Lqh III, and LqhαIT are active on hH1 channels. Superimposed whole-cell currents were recorded from HEK 293_hH1 cells at test voltages between −80 and +70 mV in 10-mV increments in the absence (left) and presence (right) of 5 nM of the indicated toxins.

how much voltage change is needed for an e-fold increase in the time constants.

The association rates were assessed with a double-pulse protocol. A conditioning prepulse to very high depolarization voltages caused maximal toxin dissociation. It was followed by hyperpolarizing pulses of increasing duration to follow the time course of toxin rebinding and action. At each association voltage, the association kinetics was followed by plotting $I_{5\,ms}/I_{peak}$ versus the association durations and fitted with a single exponential to yield the time constants (τ_{on}).

RESULTS

Lqh Toxins Modify Activation and Fast Inactivation of hH1 Channels

Families of Na^+ currents from whole-cell recordings of HEK 293_hH1 cells in the absence (left) and presence (right) of 5 nM Lqh II, Lqh III, and LqhαIT are shown in Fig. 1. Although under control conditions hH1 channels inactivate rapidly and completely, Lqh II and Lqh III at that low concentration strongly slowed down fast inactivation of hH1 channels. At 100 nM, LqhαIT also had a considerable effect of fast inactivation of these channels (see below).

From data like those shown in Fig. 1, but in the absence and presence of 100 nM toxins, current-voltage relationships and voltage dependencies of steady-state fast inactivation were compiled and analyzed with Eqs. 1 and 2, respectively. The resulting parameters for

TABLE I

Parameters for the Activation and Steady-state Fast Inactivation of hH1 Channels

	Activation			Fast inactivation			
	V_m	k_m		V_{hf}	k_{hf}	a_{DC}	
	mV	*mV*	*n*	*mV*	*mV*	%	*n*
Control	−52.9 ± 1.5	12.3 ± 0.2	12	−88.1 ± 2.0	5.4 ± 0.1	1.0 ± 0.3	11
Lqh II	−58.1 ± 1.7*	14.4 ± 0.4*		−95.8 ± 2.3*	8.5 ± 0.2*	5.6 ± 0.8*	
Control	−47.7 ± 3.2	12.8 ± 0.5	8	−84.1 ± 2.9	5.2 ± 0.1	0.6 ± 0.2	7
Lqh III	−52.2 ± 3.5‡	15.3 ± 0.7*		−89.1 ± 3.4*	8.6 ± 0.3*	5.8 ± 0.7*	
Control	−54.6 ± 1.5	12.3 ± 0.4	10	−89.9 ± 2.1	5.5 ± 0.3	0.6 ± 0.2	9
LqhαIT	−60.7 ± 1.7*	13.7 ± 0.5*		−96.5 ± 2.1*	8.6 ± 0.3*	3.5 ± 0.7*	

Parameters of activation and inactivation of hH1 channels in the absence and presence of 100 nM of the indicated toxins.
*t test: $P < 0.01$.
‡t test: $0.01 < P < 0.05$.

channel activation and fast inactivation are shown in Table I. All three toxins at 100-nM concentration shifted the threshold of channel activation by about −5 mV and slightly increased the slope factors of activation without changing the reversal potential (not shown). The toxins only slightly increased the maximal inward Na^+ currents through hH1 channels (0–30%), whereas they largely increased the peak inward currents in current-voltage relationships of μI channels (30–70%; Chen et al., 2000). Lqh II, Lqh III, and LqhαIT shifted the steady-state inactivation in hH1 channels by only about −6 mV. However, they caused a decrease in voltage dependence of inactivation due to significantly increasing the slope factors of fast inactivation from ∼5.5 to ∼8.5 mV (Table I).

To quantify the functional effects of the toxins on hH1 channels, experiments with various toxin concentrations were performed. The average values of the ratio $I_{5\,ms}/I_{peak}$ (Fig. 2 A) from several experiments were plotted as a function of test voltages for the indicated toxin concentrations (Fig. 2 B, Lqh II). In the control, fast inactivation of hH1 channels after 5 ms increases with increasing test voltage, and is complete at ∼0 mV. This clearly indicates that the fast inactivation is strongly voltage dependent. Increasing toxin concentrations gradually reduced the voltage dependence of fast inactivation. The dose dependence of inactivation removal was analyzed at 0 mV (framed data points in Fig. 2 B). The fits of the resulting dose-response curves (Fig. 2 C) according to Eq. 4 yielded the EC_{50} values 11.5 ± 2.5 nM, 2.5 ± 0.1 nM, and 32.9 ± 5.0 nM, and the a_1 values of 0.87 ± 0.03, 0.89 ± 0.01, and 0.83 ± 0.04 for Lqh II, Lqh III, and LqhαIT, respectively. The data obtained for Lqh III on hH1 channel should be considered an operational estimate of the upper limit. Owing to the very slow onset of block (see below), no steady-state conditions could be

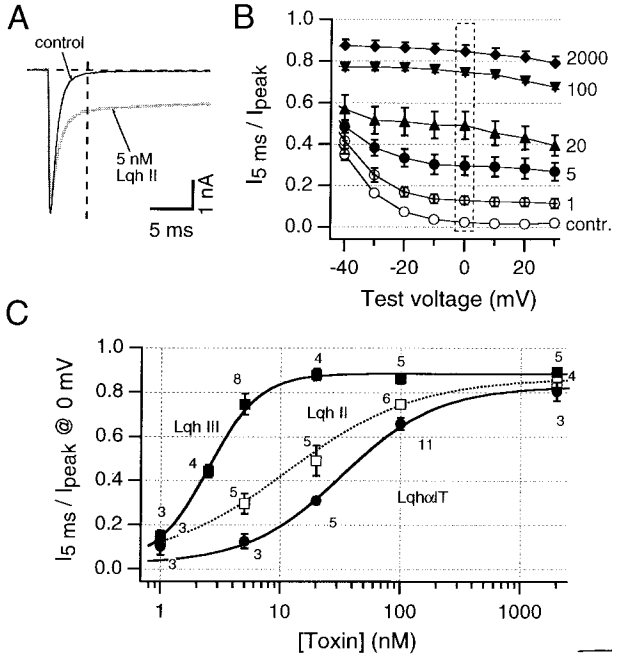

FIGURE 2. The degree of toxin-induced loss of fast inactivation is dose dependent. The ratio $I_{5\ ms}/I_{peak}$ (A) was chosen as a parameter for the degree of removing fast inactivation by toxins. (B) $I_{5\ ms}/I_{peak}$ in the absence and the presence of the indicated concentrations of Lqh II was plotted versus test voltages. Straight lines connect the data points. (C) $I_{5\ ms}/I_{peak}$, obtained at 0 mV test voltage (framed data points of B), was plotted versus the concentrations of Lqh II, Lqh III, and LqhαIT. Data were fitted according to Eq. 4 (continuous lines) yielding the following: for Lqh II, $a_1 = 0.865 \pm 0.034$, $EC_{50} = 11.5 \pm 2.5$ nM, and $h = 0.82 \pm 0.08$; for Lqh III: $a_1 = 0.885 \pm 0.012$, $EC_{50} = 2.5 \pm 0.1$ nM, and $h = 2.04 \pm 0.24$; and for LqhαIT: $a_1 = 0.826 \pm 0.044$, $EC_{50} = 32.9 \pm 5.0$ nM, $h = 1.10 \pm 0.15$. The number of experiments for each point is indicated. contr., control.

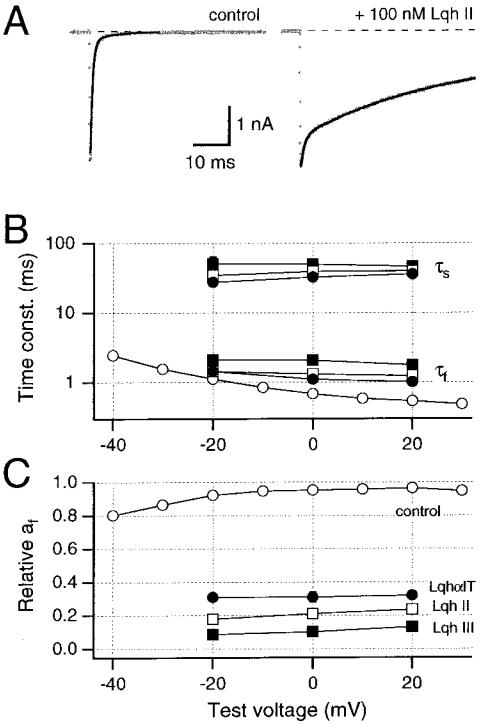

FIGURE 3. Voltage dependence of fast inactivation kinetics in hH1 channels. (A) Current traces elicited by depolarizations to 0 mV before and after application of 100 nM Lqh II. The continuous superimposed curves are the results of double-exponential data fits (Eq. 3). (B) Voltage dependence of time constants for fast inactivation kinetics in control conditions ($n = 22$; ○) and in the presence of 100 nM Lqh II ($n = 6$; □), Lqh III ($n = 5$; ■), and LqhαIT ($n = 11$; ●). (C) Relative amplitudes of the fast components ($a_f/[a_{DC}+a_f+a_s]$). Straight lines connect the data points. const., constant.

obtained at very low concentrations. Therefore, the EC_{50} value is overestimated. By the same argument, the Hill coefficient of 2.04 ± 0.24 for Lqh III will be overestimated as well, whereas the dose dependencies of Lqh II and LqhαIT obeyed more realistic Hill coefficients of 0.82 ± 0.08 and 1.10 ± 0.15, respectively. Compared with the results obtained for the other two toxins and also for the toxin interaction with μI sodium channels (Chen et al., 2000), the interaction between hH1 and Lqh III shows unusual properties.

The time course of fast inactivation in hH1 channels in the absence and presence of the toxins was analyzed using double-exponential functions (Fig. 3 A and Eq. 3). The two time constants (Fig. 3 B) and the relative amplitudes of the fast components (Fig. 3 C) were plotted versus test voltages. Under control conditions, the fast component was >90% at test voltages higher than −30 mV, and its time constant showed a clear voltage dependence (Fig. 3 B, open circles). In the presence of 100 nM of the toxins, the time constants of the slow components of fast inactivation displayed no voltage dependence at test voltage above −20 mV, whereas time constants for fast components appeared to retain much less voltage dependence than under control conditions. At the test voltage of 0 mV, the time constants of slow components were 39 ± 3, 50 ± 9, and 33 ± 3 ms for Lqh II, Lqh III, and LqhαIT, respectively. Compared with a control value of 0.68 ± 0.01 ms, time constants of fast components were 1.3 ± 0.1, 2.1 ± 0.4, and 1.1 ± 0.1 ms for the toxins. Compared with the control value of 95 ± 1%, the relative contributions of the fast components at 0 mV were about 20 ± 2, 10 ± 2, and 31 ± 3% for Lqh II, Lqh III, and LqhαIT, respectively. Thus, Lqh III not only removes fast inactivation of hH1 channels at lower concentrations, but also slows down inactivation more extensively than the other two toxins tested.

Toxin Association and Dissociation in hH1 Channels

After obtaining stable toxin effects at a concentration of 100 nM, toxin dissociation rates in hH1 channels were obtained in a voltage range from +20 to +180 mV with protocols like that shown in Fig. 4 A. As shown in Fig. 4 (B and C) a 100-ms dissociation pulse to +120 mV almost completely removed the effects of 100 nM

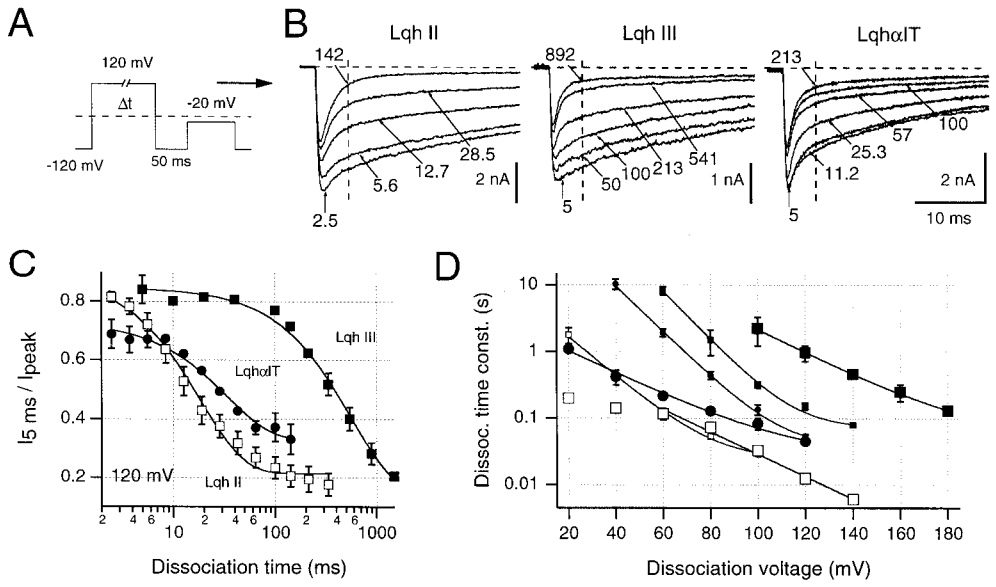

FIGURE 4. Voltage dependence of toxin dissociation from hH1 channels. (A) Pulse protocol. (B) Superimposed current traces for a toxin-dissociation experiment in the presence of 100 nM Lqh II, Lqh III, and LqhαIT. Currents were measured after conditioning pulse steps to +120 mV with increasing duration and a 50-ms return to −120 mV to recover from fast inactivation. The superimposed traces show the acceleration of fast inactivation due to toxin dissociation with longer conditioning pulses (durations are indicated in ms). Interval for each pulse is 20 s for Lqh II and LqhαIT and 30 s for Lqh III. (C) Kinetics of dissociation of the indicated toxins from hH1 channels at +120 mV dissociation potential. The ratio $I_{5\ ms}/I_{peak}$ was plotted versus the logarithm of the dissociation time and the indicated fit curves were obtained using single-exponential functions, yielding dissociation time constants (τ_{off}). Similar experiments were performed for other voltages. (D) The dissociation (Dissoc.) time constants were plotted as a function of the dissociation voltage (large symbols, n = 4–5). Also shown are data for μI skeletal muscle sodium channels (Chen et al., 2000; small symbols). The superimposed single-exponential fits to the high voltage data points yielded the increases in voltage that are needed to accelerate toxin dissociation e-fold.

Lqh II and LqhαIT on fast inactivation of hH1 channels, whereas a 540-ms dissociation pulse to the same voltage only partially removed the effects of Lqh III on fast inactivation. At the same dissociation voltage, the toxins exhibited quite different dissociation time constants in hH1 channels with the order τ_{off} (Lqh II) < τ_{off} (LqhαIT) ≪τ_{off} (Lqh III), e.g., at dissociation voltage +100 mV, τ_{off} values were 27, 84, and 2,010 ms. As a consequence, in the explored voltage range, equivalent dissociation rates are obtained for Lqh III at voltages ~140 mV higher than for Lqh II.

For each toxin, the dissociation rates were strongly voltage dependent with more depolarized voltages significantly accelerating the dissociation rate. In the high

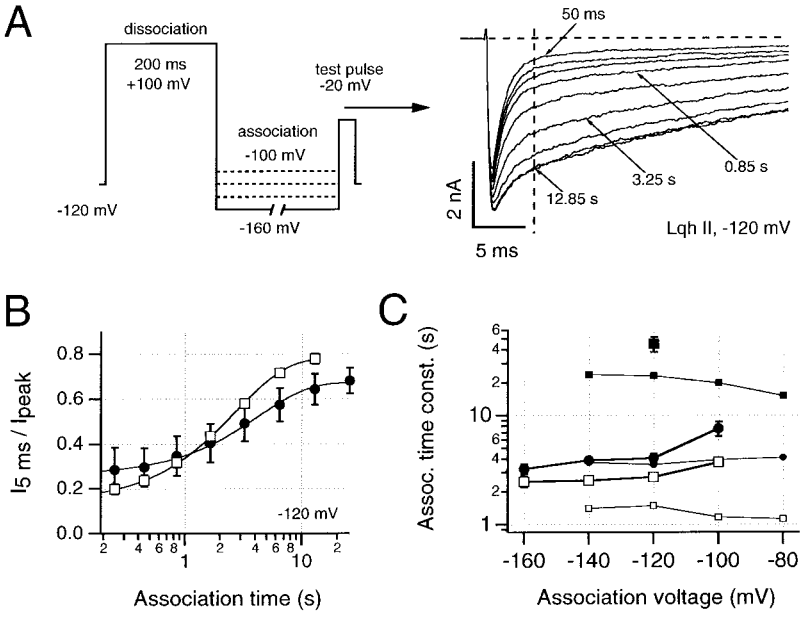

FIGURE 5. Toxin association kinetics in hH1 channels. (A) Superimposed current traces for a toxin-association experiment at association voltage −120 mV in the presence of 100 nM Lqh II. As indicated by the protocol, a 200-ms depolarizing step to +100 mV was used to dissociate most of the bound Lqh II. For the rebinding of the toxin, the membrane potential was subsequently returned to −120 mV. The superimposed current traces show the slowing of fast inactivation due to the rebinding of Lqh II with increasing periods at −120 mV (50 ms to ~13 s). (B) The kinetics of toxin association was assayed by measuring the ratio $I_{5\ ms}/I_{peak}$, here plotted versus the association time at −120 mV for Lqh II (□) and LqhαIT (●). Fits were performed with single exponentials. (C) The association (Assoc.) time constants (const.) were obtained in a voltage range from −160 to −100 mV for Lqh II and LqhαIT, and then plotted versus the association voltage (n = 3–5). The single data point (■) for the association rate of 100 nM Lqh III was measured by rapid toxin application (see Fig. 6). As a control, association rates for μI skeletal muscle sodium channels are indicated (from Chen et al., 2000; small symbols).

voltage limit, single-exponential fits yielded slope factors of 25.9 ± 1.4, 24.8 ± 8.0, and 25.8 ± 2.0 mV for Lqh II, Lqh III, and LqhαIT, respectively (Fig. 4 D). Reanalysis of the dissociation data for μI channels (Chen et al., 2000; small symbols in Fig. 4 D) yielded voltage dependencies of 14.4 ± 1.1 mV (Lqh II), 11.9 ± 0.7 mV (Lqh III), and 12.7 ± 0.9 mV (LqhαIT), clearly showing that the voltage dependence of toxin dissociation is determined by the channel protein and not by the toxin.

The association time constants (τ_{on}) of 100 nM Lqh II and LqhαIT in hH1 channels were measured with protocols shown in Fig. 5 A at association voltages between −160 and −100 mV. As shown in Fig. 5 C, the association rates of Lqh II and LqhαIT were not voltage dependent in the range between −160 and −120 mV. This result is similar to that found for μI channels for Lqh II (Chen et al., 2000). However, above −120 mV, association became significantly slower.

Owing to the very slow dissociation of Lqh III, it is very complicated to completely remove this toxin from hH1 channels even at very high dissociation voltages up to +180 mV, which in most cases leads to a loss of the seal in the whole-cell configuration. Thus, it was impossible to measure systematically association rates of Lqh III in hH1 channels with standard protocols as shown in Fig. 5 A.

Therefore, we attempted to estimate the association rates of Lqh II and Lqh III in response to rapid toxin application. Toxin effects were assayed by measuring $I_{5\ ms}/I_{peak}$ at short depolarizations to −20 mV, which were applied with a repetition interval of 1 s (Lqh II) and 5 s (Lqh III), respectively. The time course of $I_{5\ ms}/I_{peak}$ after application of 100 nM of the toxins is shown for two examples in Fig. 6 A. The development of the toxin effect could be well fitted with single-exponential functions. The time constants obtained from these fits are compared with the time constants obtained by association experiments using high voltage ("V") to dissociate the toxins from the channels (Fig. 6 B, left). It is clearly seen that the time constants, obtained with these methods, are very similar for Lqh II. For Lqh III, the slow association, only roughly estimated by voltage-induced dissociation experiments, could be confirmed (45 ± 7 s).

At −120 mV, the association rates were estimated to be 3.7, 0.22, and 2.5 $\mu M^{-1}s^{-1}$ for Lqh II, Lqh III, and LqhαIT, respectively. Thus, Lqh II binds very rapidly, whereas binding of Lqh III proceeds very slowly. The expected time constants of association with 5 nM of Lqh II, Lqh III, and LqhαIT, were about 54, 900, and 80 s, respectively, defining stringent limits to the systematic evaluation of the effects of Lqh III owing to its very slow binding and dissociation kinetics. As toxin effects were usually evaluated about 30 min after toxin application, this extremely slow association of Lqh III could be the source for the apparently large Hill coefficient (Fig. 2 C) because the effect at low toxin concentrations will be underestimated.

Toxin Modulation of Slow Inactivation and Toxin Binding in hH1 Channels

The molecular source for the voltage dependence of scorpion α-toxin dissociation from Na^+ channels is not yet known. The common belief is that protein conformational changes associated with channel activation and/or fast inactivation result in a reduced toxin binding affinity, and hence toxin dissociation. However, there are additional processes linked to channel activation that may cause a reduced toxin affinity. If we compare the dissociation rates of the Lqh toxins from hH1 and μI channels, we notice that the toxins appear to bind more tightly to hH1 channels and the voltage dependence of the dissociation from hH1 channels is only about half as big as for μI channels (Fig. 4). This difference is in a way reminiscent of the difference that these two channel types show in respect to the process of slow inactivation. hH1 channels have an incomplete slow inactivation and a weak voltage dependence, whereas μI channels slow inactivate more extensively and exhibit a steeper voltage dependence (Richmond et al., 1998; O'Reilly et al., 1999). Thus, in particular because Lqh III is binding so tightly to μI and hH1 channels even at very high dissociation voltages, it

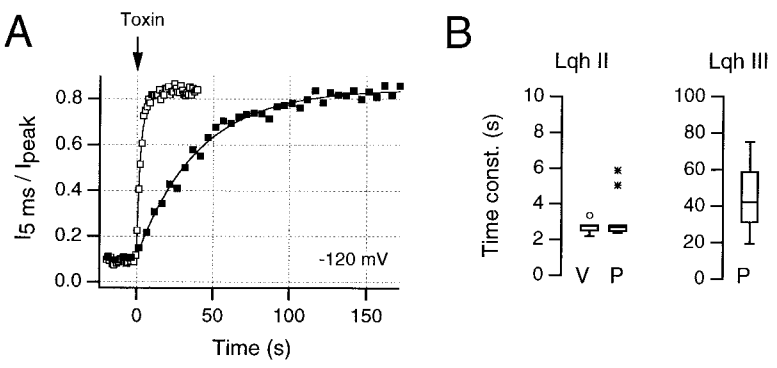

FIGURE 6. Association kinetics after rapid toxin application. (A) The degree of hH1 channel inactivation was assayed by repetitive test pulses to −20 mV with an interval of 1 s (Lqh II, 6 ms depolarization; □) or 5 s (Lqh III, 10 ms depolarization; ■). The holding voltage was −120 mV. At time zero, 100 nM of the indicated toxins were applied by an application pipet. The resulting estimates for $I_{5\ ms}/I_{peak}$ were fit with single-exponential function (superimposed). (B) The time constants (const.) for toxin association obtained from these perfusion experiments (P) are compared with those obtained from experiments shown in Fig. 5, where the toxins were dissociated from the channels by high voltage pulses (V). Presentation as box-plots; stars and circles indicate outliers.

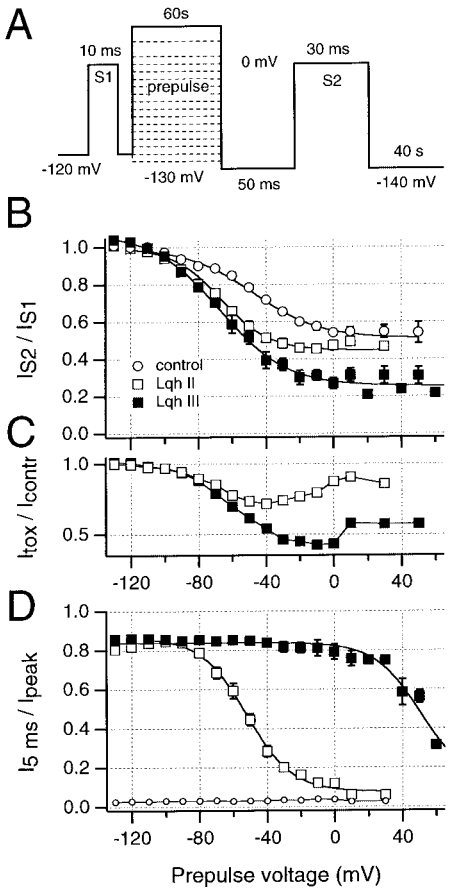

FIGURE 7. Slow inactivation and toxin binding for hH1 channels. (A) Pulse protocol used to measure "steady-state" slow inactivation and voltage dependence of toxin binding. (B) Steady-state slow inactivation without and with the 100 nM toxins. The peak current measured during pulse S2 was normalized to the peak during pulse S1 yielding the degree of slow inactivation (slow inactivation that does markedly not recover during the 50-ms pulse at −140 mV) as a function of the prepulse voltage. The continuous curves are Boltzmann fits. Both Lqh II and Lqh III enhance steady-state slow inactivation. (C) Voltage dependence of the toxin-induced increase of slow inactivation. The toxin-induced additional slow inactivation is here presented as $I_{tox}/I_{control}$, showing that the effect of Lqh II on slow inactivation is strongest at about −40 mV. (D) The degree of the remaining toxin bound was estimated by measuring $I_{5\,ms}/I_{peak}$ during the S2 pulse. Although Lqh III remains bound up to 0 mV, Lqh II nearly completely dissociates from the channel. The continuous curves are the results of Boltzmann fits with the parameters: V_h = –52.1 ± 1.1 mV and k_h = 13.5 ± 1.0 mV for Lqh II; and V_h = 51.0 ± 1.3 mV and k_h = 13.7 ± 1.3 mV for Lqh III.

should be possible to directly measure its effect on slow inactivation of these channels. As Lqh II dissociated very rapidly from hH1 channels, the effects of Lqh II on slow inactivation of hH1 channels were initially examined as a control for Lqh III.

Steady-state slow inactivation was measured with the protocol described in Fig. 7 A. In the absence of toxins, slow inactivation of hH1 channels is incomplete, i.e., a noninactivating component of 51% was measured at high voltages. Half-maximal slow inactivation was obtained at −45 mV and the voltage dependence was rather weak (20 mV per e-fold change). In the presence of 100 nM Lqh II and Lqh III, steady-state slow inactivation was significantly shifted by about −22 and −19 mV, respectively, and the slope factors were decreased (Fig. 7 and Table II), demonstrating that both toxins caused an increase in voltage dependence of slow inactivation in hH1 channels. However, the more pronounced effect was that Lqh III decreased the fraction of noninactivating channels at high potentials to 20%. The ratio of current after toxin application relative to the control values is shown in Fig. 7 C as a function of voltage. It is clearly seen that Lqh III strongly increases the extent of slow inactivation. Lqh II also increases slow inactivation, but shows a maximum in this effect at about −40 mV. The reason for this difference between Lqh III and Lqh II may arise from their different binding properties. In Fig. 7 D, the degree of fast inactivation after the slow inactivation prepulses (60 s) was analyzed and plotted as a function of the prepulse voltage. Although the inactivation remains eliminated for Lqh III at the voltages up to about +30 mV, Lqh II dissociated at a half-maximal voltage of −52.1 ± 1.1 mV with a slope factor of 13.5 ± 1.0 mV. Lqh III only dissociated at higher voltages. V_h of +51.0 ± 1.3 mV and k_h of 13.7 ± 1.3 mV were estimated based on a smaller number of additional experiments, which were complicated to perform because of the instability of whole-cell configurations during long depolarizations to high voltages. Although both toxins dissociate at high voltages, they have a significant enhancing effect on slow inactivation at physiologically relevant voltages (e.g., −70 mV), and it appears as if some of this effect remains at high voltages even after toxin dissociation has occurred.

TABLE II

Parameters for the Steady-State Slow Inactivation of hH1 and μI Channels

	V_{hs}	k_{hs}	a_{DC}	
	mV	*mV*	%	*n*
hH1 channels				
Control	−44.7 ± 0.5	20.1 ± 1.1	51 ± 2	5
Lqh II	−68.4 ± 1.1*	14.6 ± 1.6*	43 ± 4	4
Lqh III	−63.9 ± 2.2*	18.7 ± 1.9	20 ± 4*	5
μI channels				
Control	−55.3 ± 1.0	10.5 ± 0.2	28 ± 2	11
Lqh III	−63.2 ± 0.2*	7.6 ± 0.3*	21 ± 2*	6
Lqh II	−67.6 ± 5.4*	8.5 ± 0.7*	12 ± 3*	4

Parameters were determined in the absence and presence of 100 nM of the indicated toxins.
*t test: $P < 0.01$.

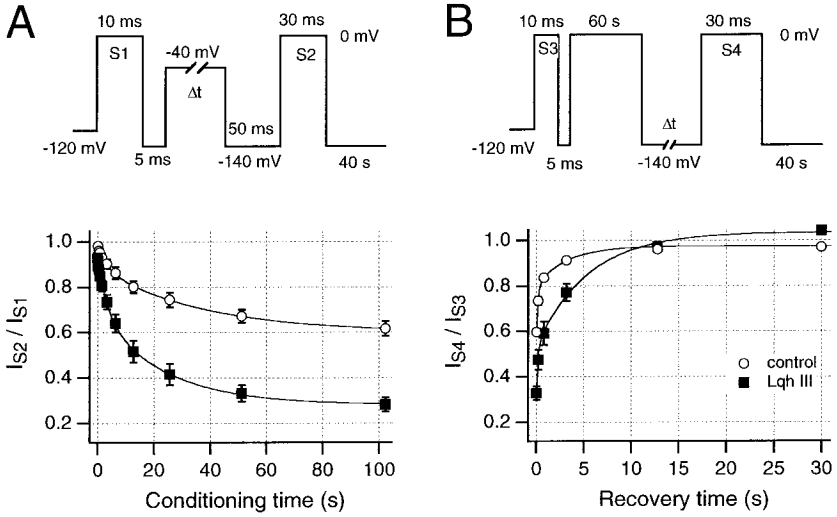

FIGURE 8. Kinetics of slow inactivation for hH1 in the presence of Lqh III. (A) Kinetics of the onset of slow inactivation at −40 mV was measured according to the indicated protocol. 100 nM Lqh III accelerated the slow inactivation. (B) Kinetics of the recovery from slow inactivation at −140 mV was also slowed down by 100 nM Lqh III. The continuous curves in A and B are double-exponential fits (see text).

Lqh III Changes the Kinetics of Slow Inactivation in hH1 Channels

As Lqh III dramatically changed steady-state slow inactivation of hH1 channels, the effects of Lqh III on the development of slow inactivation were examined with a two-pulse protocol. Fig. 8 A shows that Lqh III accelerated the development of slow inactivation and increased the fraction of hH1 channels that entered slow inactivation. In the presence of Lqh III, the short time constant was not affected (3.6 s), but the long time constant for the development of slow inactivation was significantly decreased (from 37 to 23 s at −40 mV), and the ratio for the slow component was significantly increased (from 29 to 52% at −40 mV). Moreover, steady-state slow inactivation with a 102-s depolarization pulse was significantly increased (from 42 to 72% at −40 mV).

The recovery from slow inactivation of hH1 channels in the absence and presence of 100 nM Lqh III was investigated with the protocol shown in Fig. 8 B. Lqh III did not change significantly the two time constants (τ_f, 0.22 s for control versus 0.14 s for Lqh III; and τ_s, 4.98 s for control versus 4.99 s for Lqh III) and the ratio for the fast component of recovery from slow inactivation (ratio of τ_f, 30.3% for control versus 30.5% for Lqh III). However, the ratio of the slow component was significantly increased from 17 to 49%. Thus, Lqh III slowed down the recovery rate from slow inactivation of hH1 channels mainly by influencing the amplitude of the slow component of the recovery kinetics.

Toxin Modulation of Slow Inactivation and Toxin Binding in μI Channels

To test whether the effect of Lqh toxins on slow inactivation is a general phenomenon or specific for hH1 channels, we performed similar experiments to those shown in Fig. 7 for μI skeletal muscle channels (Fig. 9). In this case, 100 nM of the toxins left shifted the voltage dependence of slow inactivation by about −10 mV and slightly increased the voltage dependence (Table II). The degree of slow inactivation was also increased. Both Lqh II and Lqh III showed a maximum relative effect on slow inactivation at around −50 to −40 mV, indicating toxin dissociation during the 60-s prepulses to high voltages. This is shown in Fig. 9 D by plotting $I_{5\ ms}/I_{peak}$ as a function of the prepulse voltage. Lqh II dissociated with a half-maximal voltage of −39.1 ± 1.8 mV and a slope of 10.8 ± 1.1 mV. Dissociation of Lqh III had to be described with a double Boltzmann function; the most prominent component being described by V_h = +28.9 ± 1.4 mV and k_h = 11.9 ± 1.1 mV. It is important to note here that Lqh II seems to have a stronger effect on slow inactivation than Lqh III, although Lqh II binds less tightly and shows much faster dissociation kinetics.

DISCUSSION

Action of Lqh α-Toxins on hH1 Channels

Lqh II, Lqh III, and LqhαIT markedly slow down the kinetics of fast inactivation in hH1 and significantly reduce the voltage dependence of steady-state fast inactivation. These are typical effects of scorpion α-toxins. The same toxins had similar effects on μI (Chen et al., 2000) and other site 3 toxins were also shown to remove inactivation and to shift its voltage dependence (Chahine et al., 1996b; Rogers et al., 1996: Benzinger et al., 1999). This similarity suggests that the toxins act by a similar molecular mechanism and bind to a common site, mostly determined by receptor site 3, i.e., the linker between segments 3 and 4 in domain D4 (see also Benzinger et al., 1997, 1998).

Although qualitatively similar, the quantitative effects of the three toxins tested on hH1 channels differ significantly from those previously reported for μI channels. The limiting time constants of fast inactivation after toxin application are >30 ms for hH1 channels, but

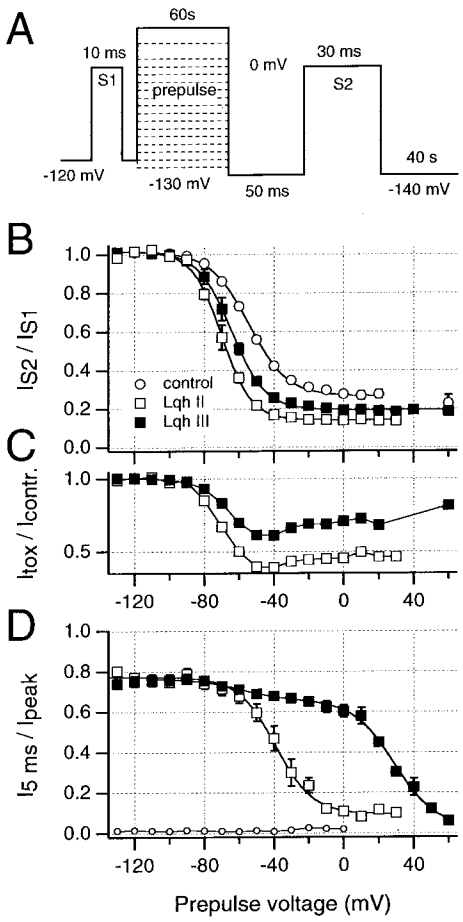

FIGURE 9. Slow inactivation and toxin binding for μI channels. (A) The pulse protocol is identical to that shown in Fig. 7 A. (B) Steady-state slow inactivation with and without 100 nM toxins. (C) Voltage dependence of the toxin-induced increase of slow inactivation. (D) The degree of the remaining toxin bound was estimated by measuring $I_{5\,ms}/I_{peak}$ during the S2 pulse. The continuous curves are the results of single (Lqh II) and double (Lqh III) Boltzmann fits. For Lqh II, $V_h = -39.1 \pm 1.8$ mV, and $k_h = 10.8 \pm 1.1$ mV; for Lqh III, $V_{h1} = -58.9 \pm 6.5$ mV, $a_1 = 0.10 \pm 0.01$, $V_{h2} = 28.9 \pm 1.4$ mV, and $a_2 = 0.63 \pm 0.03$, and a common slope factor $k_h = 11.9 \pm 1.1$ mV, where a_i is the amplitude of the respective components.

only 15 ms for μI channels. The EC_{50} values of Lqh II, Lqh III, and LqhαIT to remove fast inactivation of hH1 channels are 12, <2.5, and 33 nM, respectively, compared with those in μI channels of 1.4, 7.2, and 0.5 nM, respectively. These results show that both skeletal and heart muscle of mammals are very important targets for these three toxins. However, it also says that the three toxins tested are very useful tools for the discrimination among different channel types. Although Lqh III has the highest and LqhαIT the lowest potency on hH1 channels (separated by more than a factor of 10) for μI channels the situation is just the opposite, clearly showing that structural changes of the channel protein can result in the improvement of binding for one toxin, but simultaneously may lead to a reduced affinity of another α-toxin from the same species. Mutagenesis studies may unravel how much of these differences can be accounted for the differences in receptor site 3. Comparison of the putative receptor sites 3 indicates that there are only two residues different between hH1 and μI channels: I1611 (hH1) versus L1429 (μI) and F1617 (hH1) versus V1435 (μI). Interestingly, the site F1617 lies COOH-terminal outside a hot spot for the binding of gating modifying peptides identified for the interaction of hanatoxin with *Shaker* and DRK1 potassium channels and ω-Aga-IVA toxin with α_{1A} calcium channels (Winterfield and Swartz, 2000).

The strong effect of the Lqh toxins on human cardiac Na^+ channels may form the molecular basis for their ability of inducing cardiac arrhythmias and, therefore, their life-threatening toxicity in mammals.

Strong Interaction between hH1 and Lqh III

Although all three toxins tested slowed down the fast inactivation time course in hH1 channels, the interaction of Lqh III with hH1 channels seems to be particularly strong. In the presence of 100 nM Lqh II, Lqh III, and LqhαIT, the limiting time constants (τ_s) of the slow component of fast inactivation at test voltage 0 mV were 39, 50, and 32 ms, respectively, compared with 15 ms for all three toxins in μI channels. Thus, Lqh III is much more potent to remove fast inactivation of hH1 channels than Lqh II and LqhαIT. In addition, the amplitude of the slow component also provides information on the toxin activity to remove fast inactivation on hH1 channels, e.g., in the presence of 100 nM of Lqh II, Lqh III, and LqhαIT, the ratios of the slow component at test voltage 0 mV were much different in hH1 channels (81, 90, and 72%, respectively), but they were nearly the same (~88%) in μI channels,

The most important feature of Lqh III seems to be the exceptionally slow rates of binding and unbinding. In μI channels, both toxin association and dissociation kinetics followed the order Lqh II > LqhαIT > Lqh III, i.e., Lqh II is fast and Lqh III very slow (Chen et al., 2000). This indicated that the absolute on- and off-rates of the toxins are affected by the nature of the toxins in a similar way. The association rates of the toxins to hH1 channels followed the same sequential order, but were consistently slower compared to those for μI channels (at −120 mV, τ_{on} = 2.7 vs. 1.7 s for Lqh II; τ_{on} = 4.1 vs. 3.6 s for LqhαIT; and τ_{on} = 45 vs. 23 s for Lqh III). The very slow association rate at low Lqh III concentrations compromised a real steady-state measurement of Lqh III binding with electrophysiological methods.

The dissociation rates of Lqh II and LqhαIT from hH1 channels were faster than that from μI channels (at +100 mV, τ_{off} = 27 vs. 30.1 ms for Lqh II; and τ_{off} = 84 vs. 135 ms for LqhαIT). However, the dissociation rate of Lqh III from hH1 channels was much slower

than that from μI channels (at +100 mV, τ_{off} = 2,010 vs. 322 ms), suggesting that Lqh III binds to hH1 channels most strongly and the interaction between the hH1 channel and Lqh III is unusual.

Mechanism of Toxin–Channel Interactions

Several studies on scorpion α-toxins have shown that the toxin affinity to voltage-gated Na^+ channels is voltage dependent; upon depolarization, the toxins dissociate from the channels and fast inactivation is transiently restored (Rogers et al., 1996). However, the molecular source for this voltage-dependent toxin dissociation is not known. For those toxins that dissociate rapidly, the apparent voltage dependence of "binding" could be correlated with the activation threshold of the Na^+ channels. Thus, one may speculate that channel activation reduces the toxin's binding affinity. However, this conclusion cannot easily be supported by direct evidence because there are additional molecular processes that are coupled to the voltage-dependent activation mechanism. In the first place, this is fast inactivation, the major target of the α-toxins. But also, slow inactivation is coupled to the activation process. Thus, it remains an open question which of the factors, namely activation, fast inactivation, slow inactivation, or just the membrane voltage is the primary source for the voltage-dependence of toxin–channel interactions. Like other gating-modifier toxins acting on Na^+, Ca^{2+}, or K^+ channels by binding to extracellular regions close to the S4 segment (Li-Smerin and Swartz, 1998; Winterfield and Swartz, 2000), scorpion α-toxins bind to receptor site 3 and therefore are expected to exert the primary effects on the voltage sensor of Na^+ channels. Thus, all processes that are coupled to the conformational state of S4 may be affected by toxin binding and, in turn, may affect toxin binding.

With the results presented here we may gain some more insight into this complex question. A direct coupling of the channel activation machinery with toxin binding is feasible. However, the toxins do not alter channel activation in a strong way, and the small effects on activation threshold and slope factor could be even explained by an indirect effect due to the removal of fast inactivation. The strong interaction of toxins with fast inactivation therefore suggest that the binding affinity is reduced upon entering inactivated states. Our study adds another possibility, namely that toxin binding is coupled to slow inactivation. Although there cannot be direct proof because the toxin effect cannot be assayed in the absence of the fast inactivation gate of Na^+ channels, we may discuss several aspects that are in support of a toxin interaction with both fast and slow inactivated states.

The results about toxin association to μI (Chen et al., 2000) and hH1 channels (Fig. 5) suggest that the toxins bind to closed states of Na^+ channels. Association rates became slower for hH1 channels above −100 mV, which is consistent with a more negative threshold for activation, but also with a more negative half-maximal voltage of fast and slow inactivation compared with μI channels (Table II). The very rapid dissociation upon depolarization of some toxins may indicate that slow inactivation cannot be an important factor, because the toxin effect is relieved before slow inactivation has occurred. This argument strongly supports the importance of the state of the fast inactivation gate for the stability of the toxin–channel complex.

However, the dissociation kinetics of the toxins from hH1 channels showed a strong voltage dependence at potentials greater than +20 mV. This finding is consistent with the results on LqTx and ATX II modulation of rat brain sodium channel II (rBII; Rogers et al., 1996) and the modulation of μI channels by Lqh II, Lqh III, and LqhαIT (Chen et al., 2000). In contrast, there seems to be an apparently direct coupling of activation and toxin dissociation for the interaction of N-type calcium channels with ω-grammotoxin (McDonough et al., 1997); in this case, the dissociation rate of the toxin is not voltage dependent at potentials where channel activation is saturated.

Thus, for scorpion α-toxins the question remains regarding the source for this additional voltage dependence at high voltages. Evaluation of the voltage dependencies of toxin dissociation from hH1 channels, measured at high voltages to avoid overlap with association, revealed that all three toxins tested exhibit virtually identical voltage dependencies equivalent to ∼1 electron charge. In μI channels, Lqh II, Lqh III, and LqhαIT also display virtually identical voltage dependencies of dissociation, but equivalent to ∼2 electron charges (Chen et al., 2000). These results show that this voltage dependence is channel-isoform specific and not dependent on the nature of the toxins, although the absolute dissociation rates differ quite substantially among the toxins (Fig. 4 D). This could mean that the absolute binding strength is strongly mediated by the structure of the toxin, but is subject to a voltage-dependent modulation, associated with voltage-dependent conformational changes of the channel protein. The major structural difference of the toxins seems to be a five-residue turn (amino acids 8–12) that has been implicated in the binding interaction with LqhαIT (Zilberberg et al., 1997; Gordon et al., 1998; Krimm et al., 1999).

In particular, the toxins tested here dissociate quite slowly from hH1 and μI channels. Thus, it is conceivable that there is a correlation between slow molecular conformational changes, e.g., associated with the slow component of slow inactivation (Fig. 8 A), and toxin binding stability. Interestingly, the slope factors for the voltage dependence of slow inactivation differ between

μI and hH1 channels in a similar way as the voltage dependencies of toxin dissociation. This argues in favor of a participation of processes linked to slow inactivation in the dissociation of toxins. The binding of the toxins to receptor site 3, which is mainly formed by the S3-4 loop of D4, may in turn change the voltage dependence of slow inactivation of Na^+ channels as shown in Figs. 7 B and 9 B.

Owing to the particularly slow dissociation rate of Lqh III, the apparent binding curves (Figs. 7 D and 9 D) may deviate quite strongly from those obtained for Lqh II. Although Lqh II can dissociate within the 60-s prepulse after induction of the corresponding trigger, i.e., a combination of fast and slow inactivation, 60 s are not long enough to allow for Lqh III dissociation at low voltages. Only upon stronger depolarization to +50 mV (hH1) or +30 mV (μI) do the rate constants (see Fig. 4 D) become fast enough to ensure appreciable toxin dissociation during 60-s prepulses.

Toxin Modulation of Slow Inactivation

As shown in Figs. 7–9, Lqh II and Lqh III enhance slow inactivation of hH1 and μI channels. These results can be explained by direct or indirect effects of the toxins on slow inactivation.

An indirect effect of scorpion α-toxins on slow inactivation of Na^+ channels is expected, as fast and slow inactivation seem to be coupled (Vedantham and Cannon, 1998). According to this hypothesis, removal of fast inactivation should increase slow inactivation and, hence, α-toxins should indirectly enhance slow inactivation. In fact, recent reports showed that slow inactivation of Na^+ channels can be enhanced when fast inactivation was removed by inducing mutations in the fast inactivation structure (IFM motif replaced by QQQ; Featherstone et al., 1996; Richmond et al., 1998). Therefore, toxin-induced removal of fast inactivation will consequently enhance slow inactivation.

In addition to the indirect effect by means of a coupling to fast inactivation, the toxins may directly affect slow inactivation. There are several lines of evidence supporting such a direct mechanism. An entirely indirect mechanism would not easily explain why the toxins reduce the voltage dependence of steady-state fast inactivation (Table I) but increase the voltage dependence of steady-state slow inactivation (Table II). In addition, 100 nM of Lqh II and Lqh III are expected to have substantial and largely similar effects on fast inactivation. As a consequence, one would expect a similar effect on slow inactivation when mediated by the indirect mechanism. However, this is not the case, as Lqh III has a stronger effect than Lqh II in hH1 channels and the opposite was observed for μI channels. A pure indirect mechanism would also fail to explain the persistence of the augmentation of slow inactivation at high voltages (Figs. 7 C and 9 C), i.e., at voltages where toxins substantially have lost their effect on fast inactivation (Figs. 7 D and 9 D).

Thus, besides the obvious indirect effect on slow inactivation by removal of fast inactivation, the α-toxins tested seem to directly affect slow inactivation by an alternative mechanism. Obviously, the ultimate direct test would be to test the toxin effects on slow inactivation of mutant channels in which fast inactivation is impaired (e.g., IFM-QQQ mutation in the linker between D3 and D4). However, in our hands these mutants, both in the background of hH1 and μI channels, did not yield strong enough expression to allow for faithful measurements of slow inactivation.

With this study, we intended to evaluate the effect of Lqh III on slow inactivation of hH1 channels, as we found that Lqh III binds to hH1 channels so tightly such that strong depolarizations, which are needed to induce slow inactivation, cannot completely dissociate Lqh III from these channels. As Lqh II dissociates so rapidly from hH1 channels, it was originally considered a control for Lqh III. Surprisingly, Lqh II also augments slow inactivation of hH1 and μ1 channels. This suggests that it is a common property of scorpion α-toxins to regulate slow inactivation of Na^+ channels, even if they only bind rather weakly to Na^+ channels such as LqTx to rBII channels (Rogers et al., 1996).

Toxin Effects on Peak Sodium Current

Typically, scorpion α-toxins or other site 3–specific toxins slightly increase or decrease the peak currents of Na^+ channels (Gordon, 1997). ATX II and LqTx did not change much the peak currents of rBII channels (Rogers et al., 1996), and ATX II did not change much the peak currents of μI and hH1 channels either (Chahine et al., 1996a). The results presented here showed that Lqh II, Lqh III, and LqhαIT did not change much the peak currents of hH1 channels. However, Lqh II, Lqh III, and LqhαIT strongly increased the peak currents of μI channels by increasing the maximal channel open probability (Chen et al., 2000). Even a partial sequential coupling of activation and fast inactivation would predict an increase in peak current upon removal of fast inactivation. However, this effect is counteracted by a simultaneous increase in steady-state slow inactivation. Depending on the holding voltage and the channel type, the combination of both effects may result in increases or decreases of the peak current. In the case of hH1 channels, the effect on slow inactivation seems to compensate for the removal of inactivation because of the small voltage dependence of steady-state slow inactivation that leads to an effect even at fairly negative holding voltages (see Fig. 7 B). In comparison, for μI channels the effect of an altered slow inactivation is negligible around a typical holding voltage (see Fig. 9 B) and, thus, the peak current increase in-

duced by the removal of fast inactivation dominates. Such effects on peak current can be eliminated when considering that application of α-toxins may increase the slow inactivation and slow down recovery from slow inactivation. Therefore, the validity of repetition intervals and the positioning of p/n leak pulses has to be carefully checked in the presence of toxin.

Physiological Significance

The effects of Lqh II and Lqh III on slow inactivation of Na^+ channels (μI, hH1) may play very important roles in the toxicity of scorpion α-toxins on mammals. The toxins kill animals by inducing paralysis and/or cardiac arrhythmias. This results from removing the fast inactivation of Na^+ channels and prolonging the action potentials of excitable cells, but their effects on slow inactivation and their voltage-dependent binding properties have not yet been considered. In particular, at physiological resting potentials of −70 to −80 mV, the increase of slow inactivation induced by scorpion α-toxins will reduce the number of available Na^+ channels in excitable cells. This decreases the excitability and protects the cells. In addition, long depolarizations induced by scorpion α-toxins in excitable cells will partially dissociate the toxins from Na^+ channels because of their voltage-dependent binding properties, leading to a reduced total toxin effect. In this respect, Lqh III is particularly suited in affecting cardiac function, as it remains bound to hH1 channels during the long cardiac action potentials. In summary, the impact of α-toxins on excitable cells may be overestimated when only considering their primary effect on fast inactivation under voltage-clamp conditions and very negative holding voltages.

The authors would like to thank A. Rossner, S. Arend, and E. Leipold for technical assistance. We thank A.L. George Jr. for providing the pRC/CMV-hH1 cDNA clone, J. Trimmer for providing the coding sequence of μI channels, and D. Gordon for providing Lqh II.

Submitted: 2 October 2000
Revised: 5 March 2001
Accepted: 9 April 2001

REFERENCES

Balser, J.R., H.B. Nuss, N. Chiamvimonvat, M.T. Perez-Garcia, E. Marban, and G.F. Tomaselli. 1996. External pore residue mediates slow inactivation in μ1 rat skeletal muscle sodium channels. *J. Physiol.* 494:431–442.

Benzinger, G.R., C.L. Drum, L.Q. Chen, R.G. Kallen, and D.A. Hanck. 1997. Differences in the binding sites of two site-3 sodium channel toxins. *Pflügers Arch.* 434:742–749.

Benzinger, G.R., J.W. Kyle, K.M. Blumenthal, and D.A. Hanck. 1998. A specific interaction between the cardiac sodium channel and site-3 toxin anthopleurin B. *J. Biol. Chem.* 273:80–84.

Benzinger, G.R., G.S. Tonkovich, and D.A. Hanck. 1999. Augmentation of recovery from inactivation by site-3 Na^+ channel toxins. *J. Gen. Physiol.* 113:333–346.

Catterall, W.A. 1992. Cellular and molecular biology of voltage-gated sodium channels. *Physiol. Rev.* 72:S15–S48.

Chahine, M., I. Deschene, L.Q. Chen, and R.G. Kallen. 1996a. Electrophysiological characteristics of cloned skeletal and cardiac muscle sodium channels. *Am. J. Physiol.* 271:H498–H506.

Chahine, M., E. Plante, and R.G. Kallen. 1996b. Sea anemone toxin (ATX II) modulation of heart and skeletal muscle sodium channel alpha-subunits expressed in tsA201 cells. *J. Membr. Biol.* 152:39–48.

Chen, H., D. Gordon, and S.H. Heinemann. 2000. Modulation of cloned skeletal muscle sodium channels by the scorpion toxins Lqh II, Lqh III, and LqhαIT. *Pflügers Arch.* 439:423–432.

Cummins, T.R., and F.J. Sigworth. 1996. Impaired slow inactivation in mutant sodium channels. *Biophys. J.* 71:227–236.

Eitan, M., E. Fowler, R. Herrmann, A. Duval, M. Pelhate, and E. Zlotkin. 1990. A scorpion venom neurotoxin paralytic to insects that affects sodium current inactivation: purification, primary structure, and mode of action. *Biochemistry.* 29:5941–5947.

Featherstone, D.E., J.E. Richmond, and P.C. Ruben. 1996. Interaction between fast and slow inactivation in Skm1 sodium channels. *Biophys. J.* 71:3098–3109.

Gellens, M.E., A.L. George, Jr., L.Q. Chen, M. Chahine, R. Horn, R.L. Barchi, and R.G. Kallen. 1992. Primary structure and functional expression of the human cardiac tetrodotoxin-insensitive voltage-dependent sodium channel. *Proc. Natl. Acad. Sci. USA.* 89: 554–558.

Gordon, D. 1997. Sodium channels as targets for neurotoxins: mode of action and interaction of neurotoxins with receptor sites on sodium channels. *In* Toxins and Signal Transduction. Cellular and Molecular Mechanisms of Toxin Action Series. P. Lazarowici and Y. Gutman, editors. Harwood Press, Amsterdam, Netherlands. 119–149.

Gordon, D., P. Savarin, M. Gurevitz, and S. Zinn-Justin. 1998. Functional anatomy of scorpion toxins affecting sodium channels. *J. Toxicol. Toxin Rev.* 17:131–159.

Hayward, L.J., R.H. Brown, Jr., and S.C. Cannon. 1997. Slow inactivation differs among mutant sodium channels associated with myotonia and periodic paralysis. *Biophys. J.* 72:1204–1219.

Hille, B. 1992. Ionic Channels of Excitable Cells. 2nd ed. Sinauer Associates, Inc., Sunderland, MA. 607 pp.

Krimm, I., N. Gilles, P. Sautière, M. Stankiewicz, M. Pelhate, D. Gordon, and J.M. Lancelin. 1999. NMR structures and activity of a novel a-like toxin from the scorpion *Leiurus quinquestriatus hebraeus. J. Mol. Biol.* 285:1749–1763.

Li-Smerin, Y., and K.J. Swartz. 1998. Gating modifier toxins reveal a conserved structural motif in voltage-gated Ca^{2+} and K^+ channels. *Proc. Natl. Acad. Sci. USA.* 95:8585–8589.

Li-Smerin, Y., and K.J. Swartz. 2000. Localization and molecular determinants of the hanatoxin receptors on the voltage-sensing domains of a K^+ channel. *J. Gen. Physiol.* 115:673–684.

Li-Smerin, Y., D.H. Hackos, and K.J. Swartz. 1999. α-Helical structural elements within the voltage-sensing domains of a K^+ channel. *J. Gen. Physiol.* 115:33–49.

McDonough, S.I., R.A. Lampe, R.A. Keith, and B.P. Bean. 1997. Voltage-dependent inhibition of N- and P-type calcium channels by the peptide toxin ω-grammotoxin-SIA. *Mol. Pharmacol.* 52: 1095–1104.

Mitrovic, N., A.L. George, Jr., and R. Horn. 2000. Role of domain 4 in sodium channel slow inactivation. *J. Gen. Physiol.* 115:707–718.

Ong, B.-H., G.T. Tomaselli, and J.R. Balser. 2000. A structural rearrangement in the sodium channel pore linked to slow inactivation and use dependence. *J. Gen. Physiol.* 116:653–661.

O'Reilly, J.P., S.Y. Wang, R.G. Kallen, and G.K. Wang. 1999. Comparison of slow inactivation in human heart and rat skeletal muscle Na^+ channel chimaeras. *J. Physiol.* 515:61–73.

Richmond, J.E., D.E. Featherstone, and P.C. Ruben. 1997. Human Na^+ channel fast and slow inactivation in paramyotonia congen-

ita mutants expressed in *Xenopus laevis* oocytes. *J. Physiol.* 499: 589–600.

Richmond, J.E., D.E. Featherstone, H.A. Hartmann, and P.C. Ruben. 1998. Slow inactivation in human cardiac sodium channels. *Biophys. J.* 74:2945–2952.

Rogers, J.C., Y. Qu, T.N. Tanada, T. Scheuer, and W.A. Catterall. 1996. Molecular determinants of high affinity binding of alpha-scorpion toxin and sea anemone toxin in the S3-S4 extracellular loop in domain IV of the Na^+ channel alpha subunit. *J. Biol. Chem.* 271:15950–15962.

Rudy, B. 1978. Slow inactivation of the sodium channel conductance in squid giant axons. Pronase resistance. *J. Physiol.* 283:1–21.

Sautiere, P., S. Cestele, C. Kopeyan, A. Martinage, H. Drobecq, Y. Doljansky, and D. Gordon. 1998. New toxins acting on sodium channels from the scorpion *Leiurus quinquestriatus hebraeus* suggest a clue to mammalian *vs* insect selectivity. *Toxicon.* 36:1141–1154.

Swartz, K.J., and R. Mackinnon. 1997. Mapping the receptor site for Hanatoxin, a gating modifier of voltage-dependent K^+ channels. *Neuron.* 18:675–682.

Thomsen, W.J., and W.A. Catterall. 1989. Localization of the receptor site for α-scorpion toxins by antibody mapping: implications for sodium channel topology. *Proc. Natl. Acad. Sci. USA.* 86: 10161–10165.

Valenzuela, C., and P.B. Bennett, Jr. 1994. Gating of cardiac Na^+ channels in excised membrane patches after modification by alpha-chymotrypsin. *Biophys. J.* 67:161–171.

Vedantham, V., and S.C. Cannon. 1998. Slow inactivation does not affect movement of the fast inactivation gate in voltage-gated Na^+ channels. *J. Gen. Physiol.* 111:83–93.

Vilin, Y.Y., N. Makita, A.L. George, Jr., and P.C. Ruben. 1999. Structural determinants of slow inactivation in human cardiac and skeletal muscle sodium channels. *Biophys. J.* 77:1384–1393.

Wang, S.Y., and G.K. Wang. 1997. A mutation in segment I-S6 alters slow inactivation of sodium channels. *Biophys. J.* 72:1633–1640.

West, J.W., D.E. Patton, T. Scheuer, Y. Wang, A.L. Goldin, and W.A. Catterall. 1992. A cluster of hydrophobic amino acid residues required for fast Na^+-channel inactivation. *Proc. Natl. Acad. Sci. USA* 89:10910–10914.

Winterfield, J.R., and K.J. Swartz. 2000. A hot spot for the interaction of gating modifier toxins with voltage-dependent ion channels. *J. Gen. Physiol.* 116:637–644.

Zilberberg, N., O. Froy, E. Loret, S. Cestèle, D. Arad, D. Gordon, and M. Gurevitz. 1997. Identification of structural elements of a scorpion a-neurotoxin important for receptor site recognition. *J. Biol. Chem.* 272:14810–14816.